

Synthesis and Characterization of CuO/graphene oxide composite



National Institute of Technology, Rourkela

Submitted by

Smrutirekha Rout

Roll No.411PH2113

Academic year: 2012-2013

NIT, Rourkela

CERTIFICATE

This is to certify that the work in the report entitled “**Synthesis and Characterization of CuO/graphene oxide composite**” by **Smrutirekha Rout**, in partial fulfilment of Master of Science degree in PHYSICS at the National Institute of Technology, Rourkela, is an authentic work carried out by her under my supervision and guidance. The work is satisfactory to the best of my knowledge.

Supervised by

Dr. P. Mahanandia

Assistant Prof.

Department of Physics

National Institute of Technology, Rourkela

Declaration

I hereby declare that the project work entitled “**Synthesis and characterization of CuO/graphene oxide composite**” submitted to National Institute of Technology, Rourkela, is the record of an original work done by me under the guidance of Dr. Pitambar Mahanandia Assistant professor, Dept. of Physics, NIT, Rourkela and this project work has not performed the basis for the award of any degree or diploma/associate-ship/fellowship and similar project if any.

Smrutirekha Rout

Roll No. - 411ph2113

ACKNOWLEDGEMENT

I owe a debt of gratitude to Prof. Sunil Kumar Sarangi, The Director, NIT, Rourkela for his vision and foresight of this One year Project which has immensely helped all of us to get a flavor and feel of research.

I am most grateful to my Supervisor Dr. Pitambar Mahanandia, for giving me the opportunity to work on an exciting project and for his for his inspiring guidance, constructive criticism and valuable suggestion throughout the project work. I wish to record my special thanks to Mr. Bamdev Das (M.Tech), Mr. Prakash Chandra Mahakul (Ph.D) and KadambineeSa (Ph.D) for their valuable help in all respect of my project work. I would like to thank all the people who have contributed to this work.

I record my sincere thanks to Department of Metallurgical and Material Science for extending all facilities to carry out the XRD and SEM.

I express heartiest thanks to all the faculty members of Department of Physics, NIT Rourkela who have made direct or indirect contribution towards the completion of this project.

It gives me an enormous pleasure to thank all my friends and all the research scholars of the Dept. of Physics. In particular, I would like to thank my parents for their unconditional love and patience.

CONTENTS

	Page No.
Abstract	1
Chapter -1	
1.1 Introduction	2-3
1.2 Crystal Structure of CuO	3-4
1.3 Graphene Oxide	4
Chapter -2 Experimental Techniques	
2.1 Preparation of CuO	5
2.2 Flow chart: Synthesis techniques for CuO	5
2.3 Preparation of Graphene oxide	6
2.4 Preparation of CuO/Graphene Oxide	6
2.5 Flow chart: for CuO/graphene oxide composite	7
2.6 Characterization techniques	8
2.6.1 X-Ray Diffraction	8-9
2.6.2 Scanning Electron Microscope	10
2.6.3 UV-Visible Spectroscopy	10-11
Chapter –3 Result and Discussion	
3.1 XRD Analysis	12-14
3.2 SEM analysis	15-16
3.3 UV-Visible Spectroscopy analysis	17
Chapter-4 Conclusion and future work	18
References	19-20

Abstract

Copper oxide and graphene oxide composite have been prepared successfully. The prepared composite have been characterized by XRD, SEM and UV-Vis. Band gap calculation using formula $E_g = h\nu$ from UV-Vis shows a decrease in band gap. The electrical transport is also expected to increase but yet to be analysed.

CHAPTER-I

1.1 Introduction

Studies on copper oxide nanomaterial have grown substantially in recent years due to its direct band gap and intrinsic p-type behaviour together with low cost fabrication and good electrochemical properties. Copper oxide shows two types of polymorphism, namely, cuprous oxide (Cu_2O) and cupric oxide (CuO). These oxides are the two most important stoichiometric compounds in the CuO system. Pure cupric oxide is a black solid with a density of 6.4 g/cm^3 . It also has a high melting point of 1330°C and is insoluble in water. CuO is intrinsic p-type semiconductors with relatively small bandgap (1.2-1.85 eV) and show many attractive properties that can be utilized in a diversity of applications. Copper oxides are used for gas sensors for hydrogen[1] and volatile organic compounds[2] catalysis[3] and specially, cuprous oxide films were intensively researched in device applications such as photovoltaic solar cell [4] photoelectrochemical cell[5,6] and electrochromic coatings[7]. Based on its application and interesting physical properties its synthesis has become important. Therefore, a wide range of deposition techniques such as chemical vapor deposition[8] electrodeposition[9] thermal evaporation[10] sol-gel techniques[11] spray pyrolysis[12] pulsed laser deposition[13] and plasma based ion implantation and deposition[14] have been used to prepare Cu oxide. The physical and chemical properties of CuO are affected by the deposition method and its conditions. In addition, it can also be influenced on the electrical properties. Cupric oxide prepared by different methods also shows large variations in electrical properties and is shown in the table [15-19]

Preparation Method	Crystallinity	Conduction Type	Resistivity (ohm.cm)	Carrier Concentration (cm ⁻³)
Sintering	Polycrystalline	P-type	16.0	4*10 ⁸
Sputtering	Polycrystalline	P-type	10 ⁻² -- 10	
Sintering	Polycrystalline	P-type	2400 at 300 K 15 at 773 K	
CVT	Singlecrystal	P-type	2* 10 ⁻³	
CVT	Singlecrystal	P-type	10 ³	

Table No- 1.1 Electrical Properties of CuO

Another class of non metal oxide is the graphene oxide(GO). GO consists of oxidized graphene sheets (or ‘graphene oxide sheets’) having their basal planes decorated mostly with epoxide and hydroxyl groups, in addition to carbonyl and carboxyl groups located presumably at the edges. Generally, GO is electrically insulating [20,21].The aim of this project is to prepare and characterize CuO and GO composite. It is evident that the CuO is p-type semiconductor.

If it acts as an oxygen reducing agent, the oxygen could be extracted from GO and the CuO could be converted into n-type semiconductor or any other structure. The CuO and GO was prepared by solution methods.

1.2 Crystal Structure of CuO:

Copper (II) oxide belongs to the monoclinic crystal system. The space group of its unit cell is C2/c, and its lattice parameters are $a = 4.6837\text{\AA}$, $b = 3.4226\text{\AA}$, $c = 5.1288\text{\AA}$, $\alpha = 90^\circ$, $\beta = 99.54^\circ$, $\gamma = 90^\circ$. In the crystal the copper atom is coordinated by 4 oxygen atoms in an approximately square planar configuration.

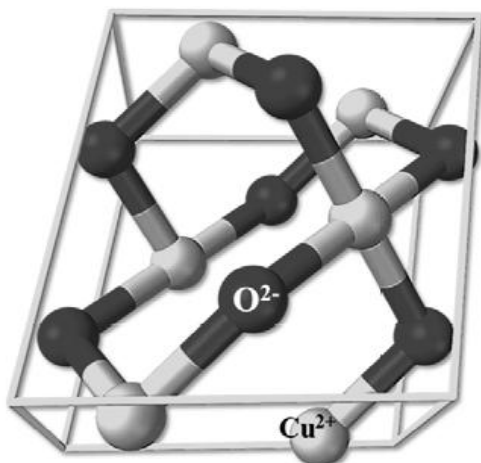


Figure 1 The Unit Cell of Copper (II) Oxide

1.3 Graphene Oxide:

Graphene has been attracting attention in recent years due to its potential for use in nanoscale devices. Graphene is a monolayer thick single sheet of graphite. The graphene sheet is the two-dimensional building block of carbon structures of all dimensions such as three-dimensional graphite, the onedimensional carbon nanotube, and the zero-dimensional buckyball.

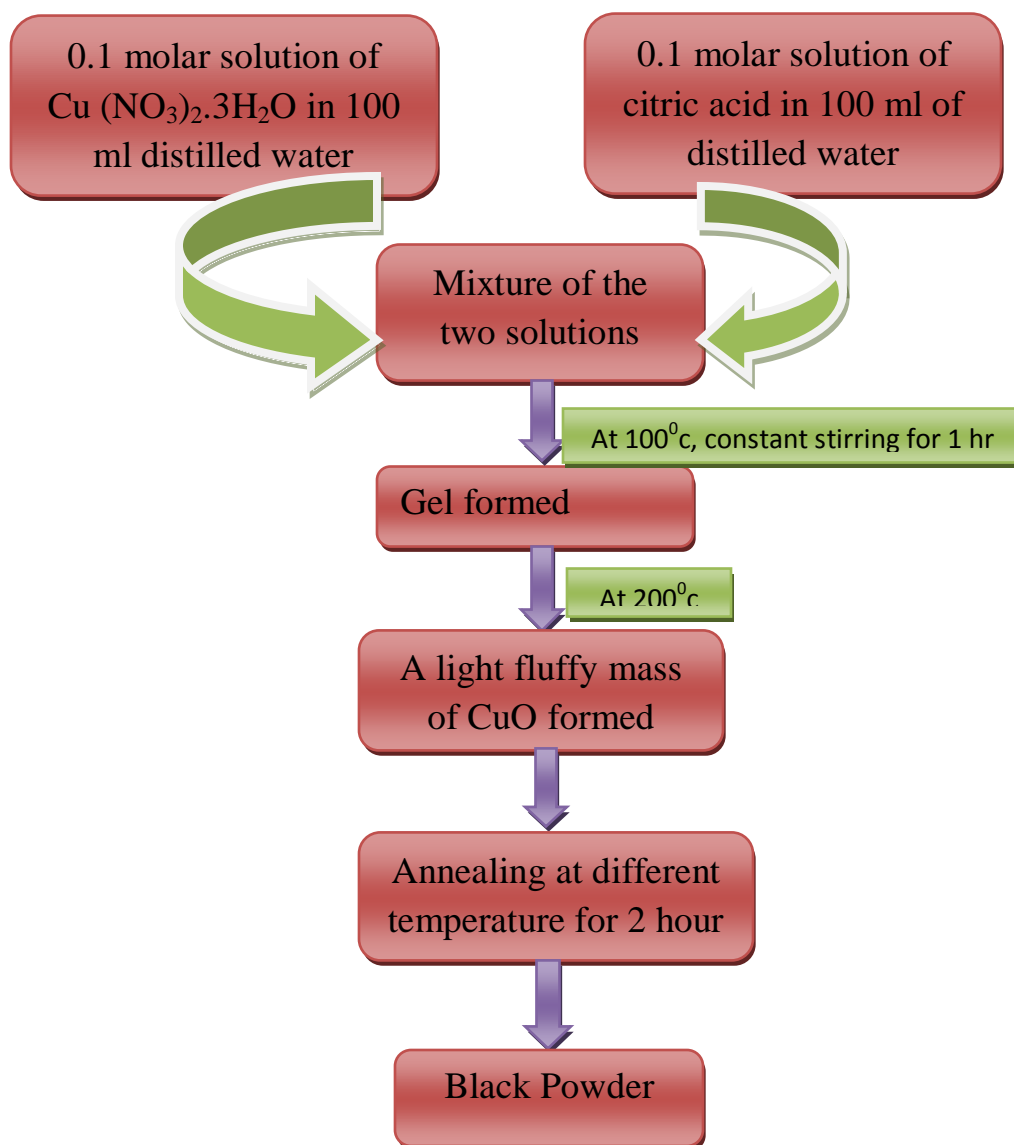
Graphene oxide (GO) is a new carbon - based nanoscale material that provides an alternative path to graphene. It is a single atomic layered material made of oxidizing graphite crystals which available in large quantities at inexpensive prices. Structurally the Graphene oxide is similar to a graphene sheet with its base having Oxygen-containing groups. These groups have a high affinity to water molecules. GO hydrophilic in nature and can be easily dissolved in water and other solvents allows it to be uniformly deposited onto wide ranging substrates in the form of thin films or networks. The basal planes and edges of the graphene oxide are functionalizing with hydroxyl, epoxy group and carbonyl groups which are attached at the edge. Then oxygen containing functional groups disturb the aromatic regions in the basal plane, so that the layer of GO consists of both aromatic regions and oxidized aliphatic six-membered rings, which leads to distorted SP^3 - hybridized geometry and results in the insulating property of GO. Graphene oxide is a poor conductor but when it treatment with heat, light or chemical reduction most of graphene's properties are restored.

CHAPTER-II

2.1 Preparation of CuO:

5 ml of the above two ($\text{Cu}(\text{NO}_3)_2 \cdot 3\text{H}_2\text{O}$ and citric acid) prepared solution and 50 ml of graphene oxide (dispersed in water) was taken in another beaker, and it was stirred about 1 hour, keeping the temperature of the material at 100°C during the process. Then the composite was annealed at 200°C for 2 hour.

2.2 Flow chart: Synthesis techniques for CuO



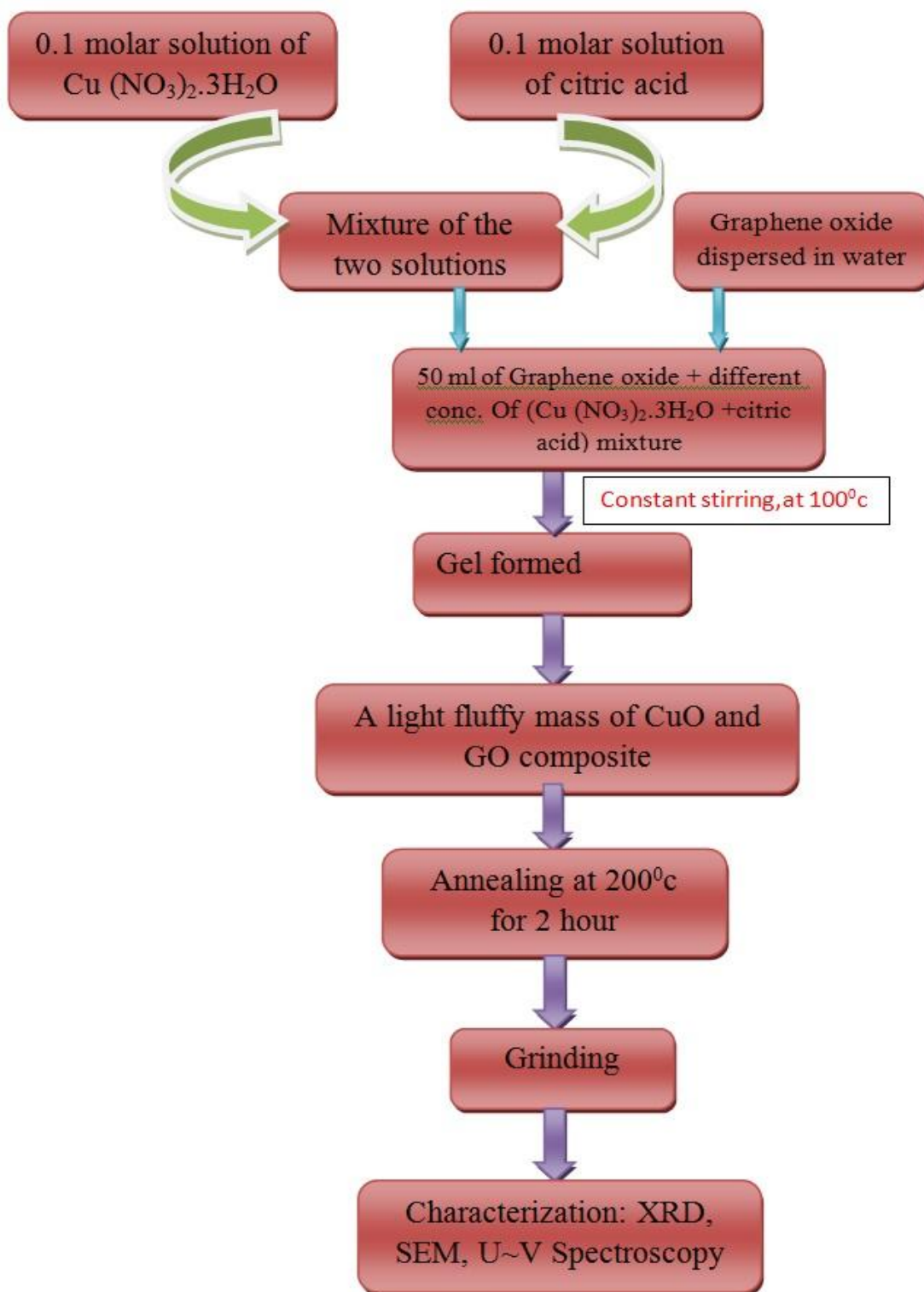
2.3 Preparation of Graphene Oxide (GO)

Similarly Go was prepared by solution method. GO is prepared firstprepared by modified Hummers' method [22,23]. In brief, GO oxide sheets were prepared from expanded graphite flakes. To exfoliate the pre-oxidized graphite powders into few layer GO sheets, the expanded graphite (EG) powder (2 g) and 15.0 g KMnO_4 was added into H_2SO_4 (120 ml) under ice-bath cooling and stirred for 2 h. The solution was diluted in DI water (250 ml), then 20 mL H_2O_2 (30%) added to it at room temperature. After precipitation for 12 h, the upper supernatant was collected and centrifuged, where the GO powders were obtained as precipitates. To remove the metal (Mn^{2+}) ions existing in the GO powders, they were dissolved in HCl solution. Finally, GO was washed many times with DI water till it reaches the PH-7.

2.4 Preparation of CuO/GO composite

5 ml of the above two ($\text{Cu}(\text{NO}_3)_2 \cdot 3\text{H}_2\text{O}$ and citric acid) prepared solution and 50 ml of graphene oxide (dispersed in water) was taken in another beaker, and it was stirred about 1 hour, keeping the temperature of the material at 100°C during the process. Then the composite was annealed at 200°C for 2 hour. The above process was repeated for CuO (10 ml)/ Graphene Oxide (50 ml).

2.5 Flow chart: for CuO/graphene oxide composite:



2.6 Characterization techniques:

There are various techniques used for characterization characterizing different nanoparticles. Here we used the basic principles of few techniques that is used in the experimental part of this project work. These are X-ray diffraction (XRD), Scanning electron microscope (SEM) and Absorption spectrophotometer (UV-VIS).

2.6.1 X-Ray Diffraction:

X-ray diffraction (XRD) is a versatile, non-destructive analytical technique which provides the information regarding the crystal structure of a substance. It gives us detail information about the lattice parameter, lattice defects, lattice strain, chemical composition, crystallite size (in case of nano particles) and the type of molecular bond of crystalline phase. The working principle of the XRD technique is simple in which a monochromatic characteristic x-rays produced by the impact of accelerated electrons with heavy metal such as Cu and which then gets filtered and collimated by nickel filters. If this x-rays beam with a characteristic wavelength λ strikes the solid with an incident angle θ then the scattered radiation is determined by Bragg's law.

The x-ray diffractometer works on the principle of Bragg's law. The general relationship between the wavelength of the incident X-rays, angle of incidence and spacing between the crystal lattice planes of atoms is known as Bragg's Law and expressed as:

$$n\lambda = 2d\sin\theta$$

Where, λ = wavelength of the incident X-rays in angstroms ((1.54 Å for copper)

d = interplanar spacing of the crystal in angstroms

θ = angle between the incident rays and surface of the crystal in degrees

n = an integer 1, 2, 3..... (Usually equal 1)

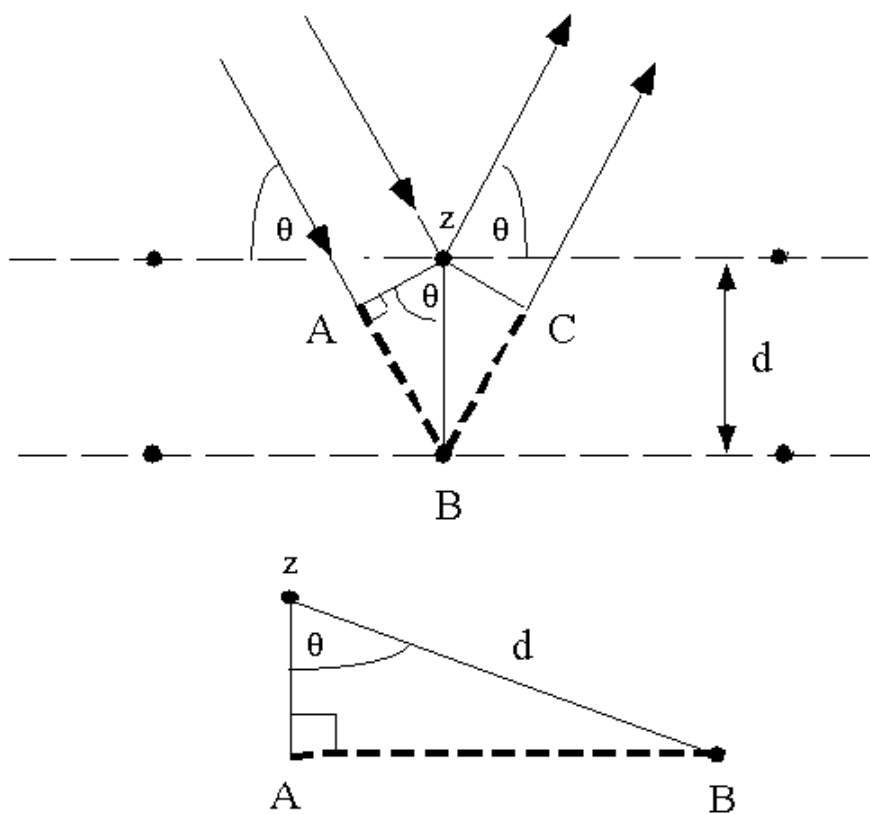


Fig 2 X-ray diffraction in accordance with Bragg's Law

The details of the XRD equipment are given below:

Equipment name	PHILIPS PW 1830 HT X-Ray Generator
Target used	Copper(Cu $K\alpha$)
Scan rate	3° per minute
Wavelength of X-ray	1.54 Å

2.6.2 Scanning Electron Microscope:

A scanning electron microscope (SEM) is a type of electron microscope that images a sample by scanning it with a high-energy beam of electrons in raster scan (step by step by the sequential scanning of the sample with the electron probe). It gives information about the sample's surface topography, morphology (crystalline structure), chemical composition, and other properties such as electrical conductivity. The SEM has a large depth of field which allows a large amount of the sample to be focus at one time and produces an image that is a good representation of the three-dimensional sample.

The Principle of SEM is an electron microscope uses an electron beam (e-beam) to produce a magnified (30,000 times magnify size) image of the sample. The important parts of a scanning electron microscope are an electron gun, a lens system, and an electron detector. The electron energy is typically 10 – 30 keV for most samples but for insulating samples the energy can be as low as several hundred eV. In SEM the working distance (distance from final lens of the microscope to the surface of the specimen) varies from 5-40 mm. In SEM long working distances give good depth of focus and short working distances give poor depth of focus. A conventional SEMs with a magnification range of 20X-30000X with spatial resolution of 50 to 100 nm.

The details of the SEM equipment are given below:

Equipment name	JEOL JSM-6480LV
Magnification	2000,....15000

2.6.3 UV-Visible Spectroscopy:

Ultra violet and visible radiation comprise only a small part of the electromagnetic spectrum which includes other forms of radiation like radio, NMR, infrared (IR), cosmic, and X rays etc. When radiation interacts with matter a number of processes can occur including reflection, scattering, absorbance, fluorescence/phosphorescence, and photochemical reaction. In general, when measuring UV-visible (UV-VIS) spectra, we want only absorbance to occur. Light

is a form of energy, absorption of light by matter causes the energy content of the molecules or atoms to increase. When light passes through a sample the amount of light absorbed is the difference between the incident radiation (I_0) and the transmitted radiation (I). The amount of light absorbed is expressed as:

$$A = -\log T$$

$$\text{Or, } A = \epsilon cb$$

Where, b =sample path length in cm

c =concentration in mol/ lit

ϵ =molar extinction coefficient in $\text{mol}^{-1}\text{cm}^{-1}$

UV-VIS spectroscopy is a non-destructive technique and a small amount of sample is required for characterize it. This technique is useful to characterize absorption, transmission, and reflectivity of different types of compounds and provides us information on the electronic bonding in a molecule.

CHAPTER- III

Result and Discussion

3.1 XRD Analysis:

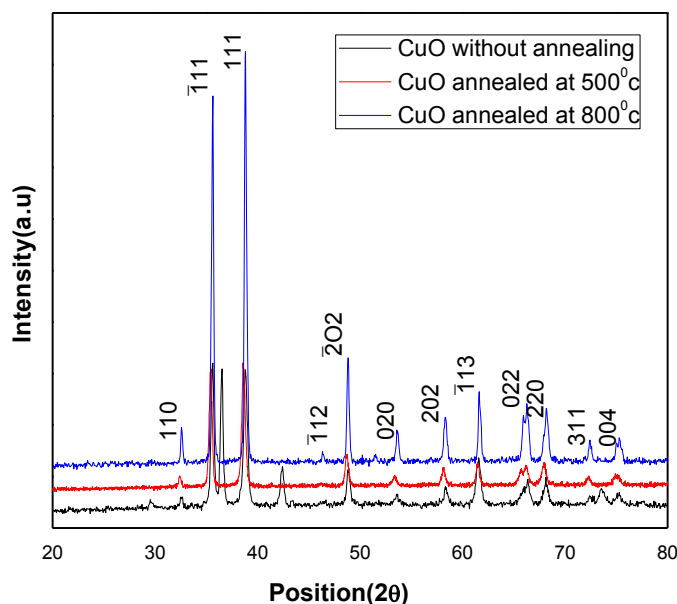
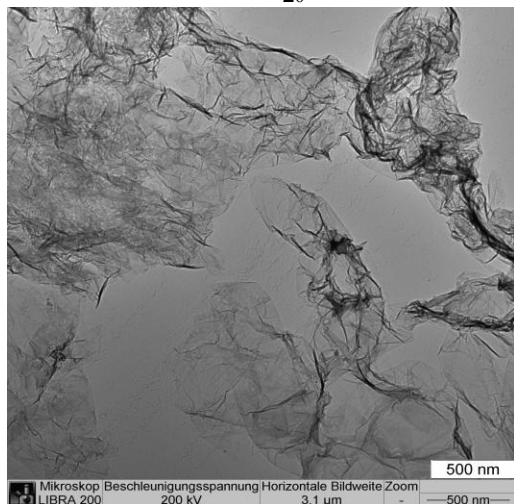
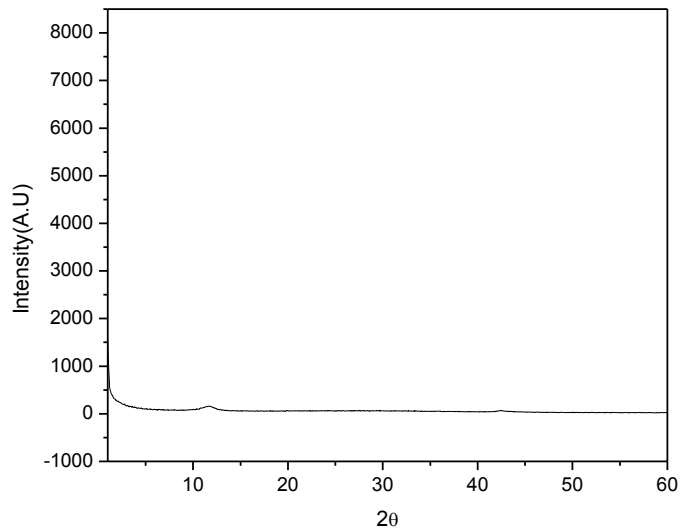
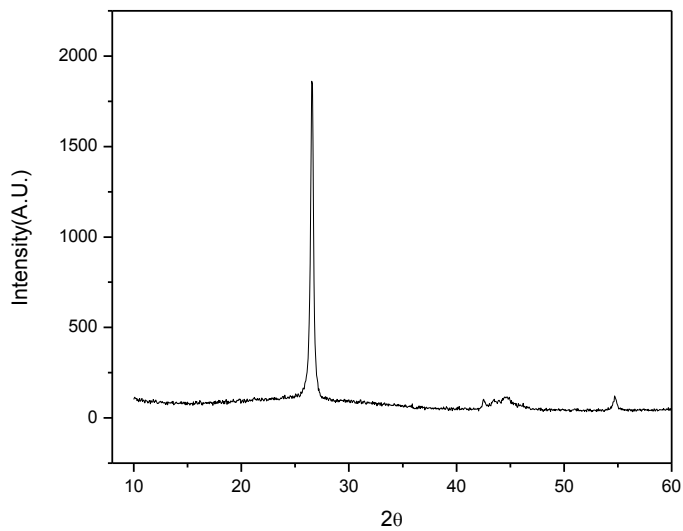
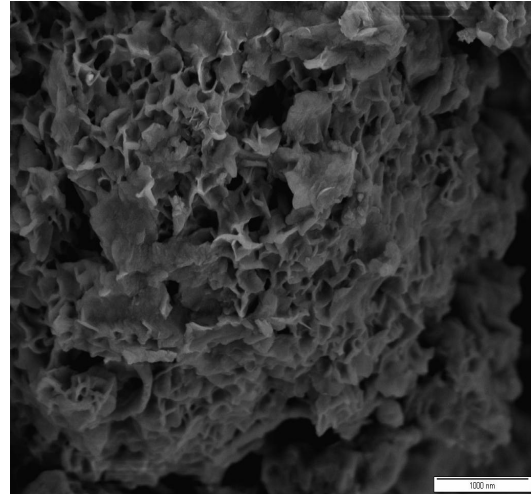
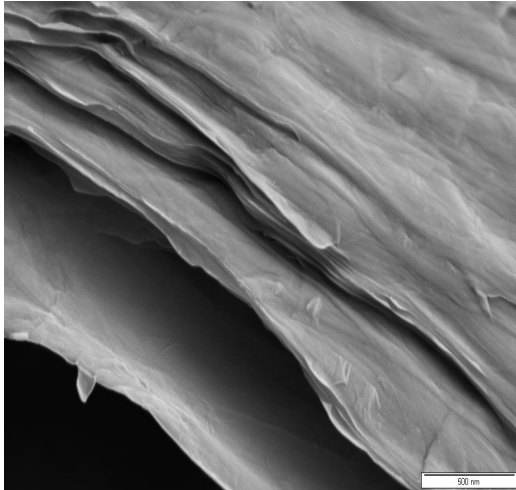


Figure 3 XRD spectra of CuO nanoparticles without annealing and annealed at 500°C, 800°C.

The typical XRD patterns of CuO nanoparticles annealed at different temperatures and their composites with graphene oxide are shown in the figure no. (3) and (4). The phase of CuO nanoparticles without annealing was perfectly matched with the International Centre for Diffraction Data (ICDD) card No 80-1268. From the XRD peaks, it was concluded that the CuO nanoparticles is crystalline in nature. The CuO nanoparticles exhibited monoclinic structure having lattice constant $a=4.6833\text{\AA}$, $b=3.4208\text{\AA}$ and $c= 5.1294\text{\AA}$.

In order to investigate the effect of temperature on CuO nanoparticles, material were further annealed at 500°C and 800°C. From the XRD peaks of CuO nanoparticles annealed at 500°C and 800°C, it is clearly shown that the intensity of peaks increases with the increase in annealing temperature which indicates that the crystallinity of CuO nanoparticles increases with

the increase of annealing temperature. Simultaneously, the peaks become narrower with the increase in annealing temperature resulting in the increase of crystallite size. The crystallite size was found to be 26.865nm and 35.2963nm for 500⁰C and 800⁰C respectively.



Figure[(4), (5), (6), (7), (8), (9)] SEM image of graphite, exfoliated GO, XRD Pattern of graphite, exfoliated GO, and TEM image of GO respectively.

The SEM image of typical graphite is shown in figure. From SEM image it is clear that how the sheets are stalked together. Figure shows the SEM image of exfoliated GO. It clearly shows that how the sheets are exfoliated and has been also confirmed by TEM. The XRD image of graphite is shown in figure. The graphitic peak (002-c axis) appears at 26.4° for graphite and other small peaks the hexagonal plane in graphene sheets. XRD of exfoliated GO is shown in figure. The XRD profile is almost flat except a small peak about 11° . This indicates that the GO is exfoliated and the small peak at 11° is due to over stalked few layers GO with more than the interlayer distance (0.335 \AA). From TEM image it is clear that the GO is exfoliated.

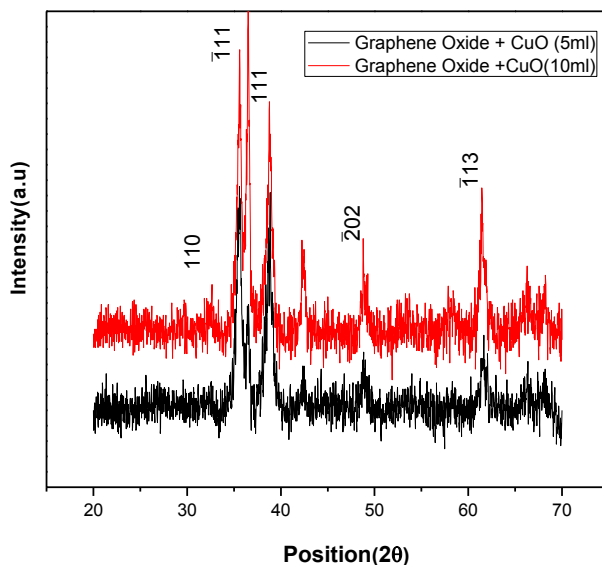


Figure 4 XRD of Graphene oxide (50 ml) /CuO (5ml) and Graphene oxide (50 ml) /CuO (10ml) annealed at 200°C

In XRD figure of CuO + Graphene Oxide composites the crystallite size of Graphene Oxide + CuO (5ml) are found to be more than Graphene Oxide/CuO (10ml) annealed at 200°C . The crystallite size was found to be 50.567nm and 41.7374 nm for Graphene Oxide + CuO (5ml) and Graphene Oxide + CuO (10ml) respectively.

3.2 SEM analysis:

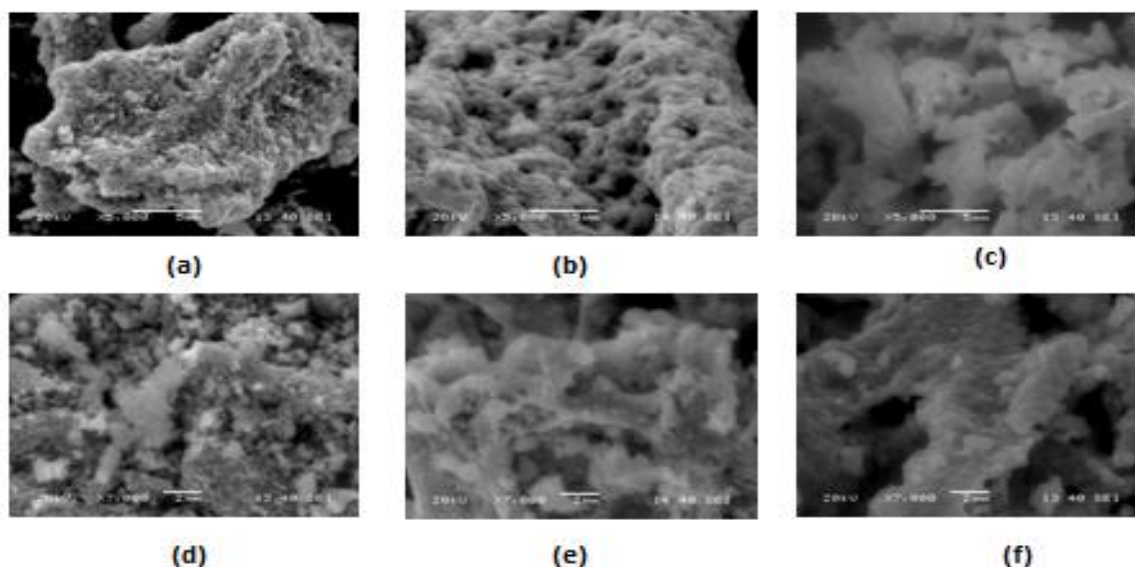


Figure 11 SEM Images of CuO nanoparticles (a), (d) without annealed (b), (e) annealed at 500⁰C (c), (f) annealed at 800⁰C having resolution 5000x and 7000x respectively.

Figure 11 shows SEM images of CuO nanoparticles at different temperature having different resolution. The SEM images [fig 11 (a), (d)] are the images of CuO nanoparticles without annealed having resolution 5000 x and 7000 x respectively. From the images, it is clearly seen that the particles are spherical in shape. The surface is not smoother. But the particle size lies well within nano range. Hence it confirms that the particles are in nano scale.

From the SEM images of CuO nanoparticles, annealed at 500⁰C [fig 11. (b), (e)], it is clearly seen that the particles are getting agglomerated and thus there is an increase in particle size. The surface of CuO nanoparticles becomes smooth. Hence there may chance to get good electrical properties.

As the CuO nanoparticles annealed at 800⁰C, the particles are agglomerated more. This agglomeration happens due to atomic diffusion. This diffusion happens due to heat treatment on

the sample. As a result the electrical properties are expected to increase than that of without annealing CuO nanoparticles.

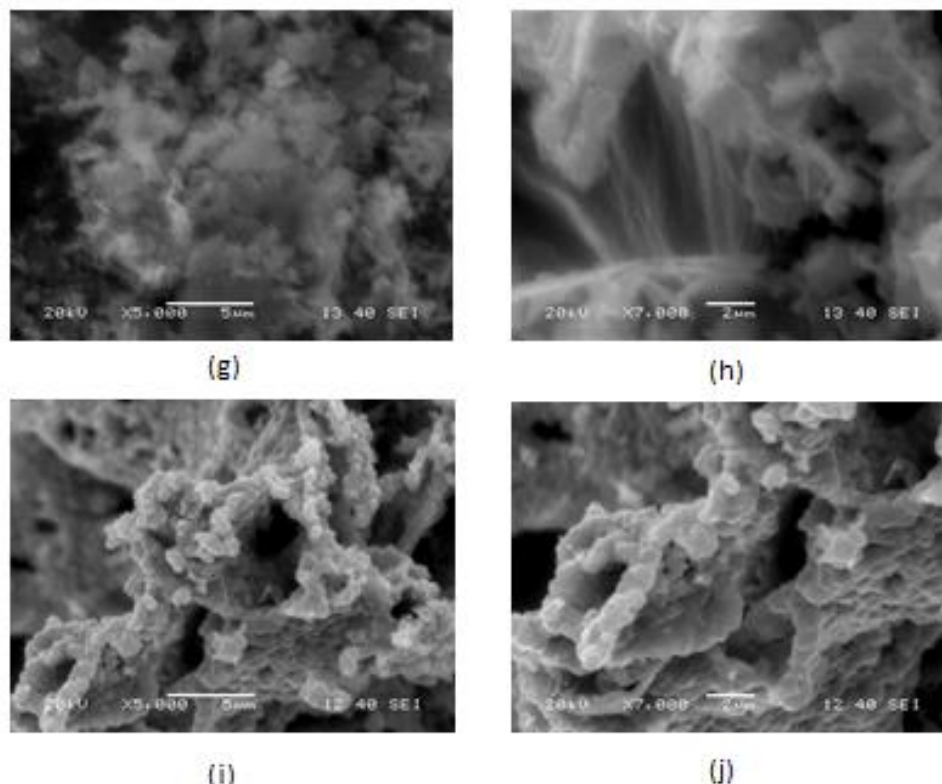


Figure 12:-SEM Images of CuO/Graphene oxide composites annealed at 200⁰C for 2 hours at two different CuO/ graphene oxide concentration i.e. 5ml of CuO solution and 10 ml CuO solution with 50 ml grapheme oxide solution which dispersed in water

Fig 12[(g), (h), (i), (j)] show the SEM images of CuO/Graphene Oxide composite having two different concentration i.e. 5 ml & 10 ml of CuO with 50 ml of graphene oxide with two different resolution 5000 x & 7000 x. From fig 12[(g), (h)], it is clear that the CuO is covering on the basal plane of the GO and hence the agglomeration is avoided. Where for the composite prepared taking 10 ml of CuO with 50 ml of graphene oxide shows the agglomeration of CuO. This may be due to higher concentration of CuO.

3.3 UV-Visible Spectroscopy analysis:

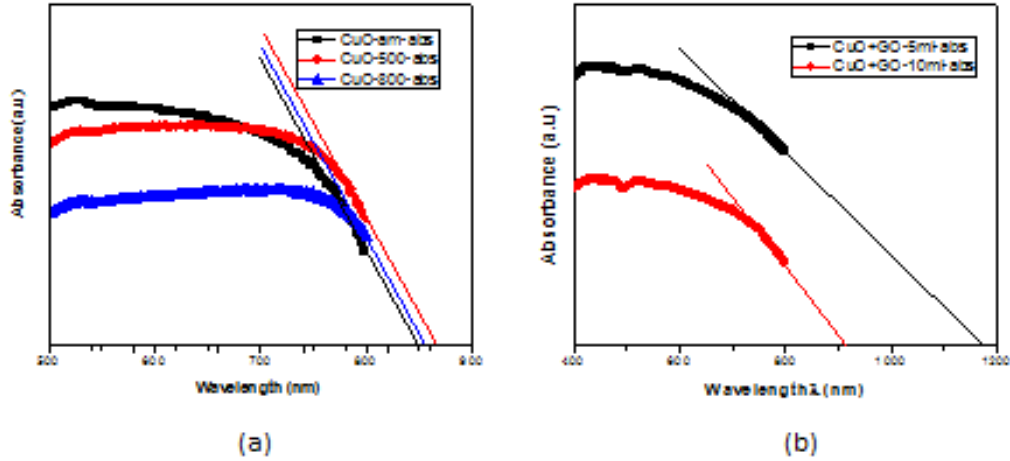


Fig 13[(a), (b)] UV-VIS Spectra of CuO nanoparticles without annealed, annealed at 500⁰C & at 800⁰C and CuO/Graphene Oxide composites at two different CuO/Graphene Oxide ratio i.e. 5ml, 10ml of CuO with 50 ml of graphene oxide.

The optical properties of CuO nanoparticles have been studied by the UV-VIS Spectrum which is shown in fig 13[(a), (b)]. From fig 13(a), it is clearly shown that the absorption spectra edge is absorbed at wavelength 850 nm for CuO nanoparticles without annealed which corresponds to energy band gap $E_g=1.4953$ eV. However, there is a temperature dependency with the UV-VIS Spectra of CuO nanoparticles annealed at different temperature i.e. at 500⁰C and at 800⁰C. From UV-VIS Spectra, it is found that the absorption spectra edge for CuO nanoparticles annealed at 500⁰C and at 800⁰C is absorbed at wavelength 866 nm and at 854 nm respectively which corresponds to energy band gap $E_g=1.43$ eV and $E_g=1.45$ eV. There is an increase in energy band with an increase in annealing temperature of CuO nanoparticles. However, in the case of CuO/graphene oxide nanoparticle, as the concentration of CuO increases from 5ml to 10 ml, the energy band increases from 1.06 eV to 1.34 eV. The absorption band edge corresponding to 5ml and 10 ml CuO with 50 ml graphene oxide is at wavelength 1169 nm and 921 nm respectively.

CHAPTER-IV

Conclusion:

Here CuO/GO composite was successfully synthesized. From the XRD figure of CuO, it was concluded that the CuO nanoparticles are crystalline in nature. Also it indicates that the crystallinity of CuO nanoparticles increases with the increase of annealing temperature. From the SEM images of CuO/Graphene Oxide composite it is clear that the CuO is covering on the basal plane of the GO and hence the agglomeration is avoided. From the UV-VIS spectra, it is seen that energy band gap increases whereas band gap decreases in case of CuO/GO composites. The reason of decrease in energy band gap is not clear at this moment.

Future Plan:

Further the electrical and transport properties of CuO/graphene oxide composite may be studied. Whether the CuO is changing from p-type to n-type in the combined system a further detailed analysis is to be carried out. Similarly, whether GO is changing into reduced GO could be analysed.

REFERENCES

- [1]. Hoa, N. D.; An, S. Y.; Dung, N. Q.; Quy, N. V.; Kim, D. Sens. Actuators B 2010, 148, 239.
- [2]Barreca, D.; Comini, E.; Gasparotto, A.; Maccato, C.; Sada, C.;Sberveglieri, G.; Tondello, E. Sens. Actuators, B 2009, 141, 270.
- [3] Medina-Valtierra, J.; Ramírez-Oriz, J.; Arroyo-Rojas, V. M.; Ruiz,F. Appl. Catal. A 2003, 238, 1.
- [4] Wong, L. M.; Chiam, S. Y.; Huang, J. Q.; Wang, S. J.; Pan, J. S.;Chim, W. K. J. Appl. Phys. 2010, 108, 033702.
- [5]Mahalingam, T.; Chitra, J. S. P.; Chu, J. P.; Moon, H.; Kwon, H. J.;Kim, Y. D. J. Mater. Sci.: Mater. Electron.2006, 17, 519.
- [6] Fernando, C. A. N.; Bandara, T. M. W. J.; Wethasingha, S. K. Sol.Energy Mater. Sol. Cells 2001, 70, 121.
- [7]Ristova, M.; Neskovska, R.; Mir eski,V. Sol. Energy Mater. Sol.Cells 2007, 91, 1361.
- [8]Markworth, P. R.; Liu, X.; Dai, J. Y.; Fan, W.; Marks, T. J.; Chang,R. P. H. J. Mater. Res. 2001, 16, 2408.
- [9] Golden, T. D.; Shumsky, M. G.; Zhou, U.; Vander Werf, R. A.;Van Leeuwen, R. A.; Switzer, J. A. Chem. Mater. 1996, 8, 2499.
- [10]Özer, N.; Tepehan, F. Sol. Energy Mater. Sol. Cells 1993, 30, 13.
- [11] Ray, S. C. Sol. Energy Mater. Sol. Cells 2001, 68, 307.

- [12]. Kosugi, T.; Kaneko, S. J. Am. Chem. Soc. 2004, 81, 3117.
- [13] Chen, A.; Long, H.; Li, X.; Li, Y.; Yang, G.; Lu, P. Vacuum 2009,83, 927.
- [14] Ma, X.; Wang, G.; Yukimura, K.; Sun, M. Surf. Coat.Technol.2007, 201, 6712.
- [15] V. F. Drobny and D. L. Pulfrey, Thin Solid Films, **61**, 89-98 (1979).
- [16] W. DeSisto, B. T. Collins, R. Kershaw, K. Dwight and A. Wold, Mat. Res. Bull., **24**, 1005-1010 (1989).
- [17] F. P. Koffyberg and F. A. Benko, J. Appl. Phys., **53**, 1173-1177 (1982).
- [18] S. Jung and H. Yanagida, Sens. Actuators, **B 37**, 55-60 (1996).
- [19] X. G. Zheng, M. Suzuki and C. N. Xu, Mat. Res. Bull., **33**, 605-610 (1998).
- [20] D.W. Boukhvalov, M. I. Katsnelson. J.Am. Chem. Soc .2008;130(32):10697–701.
- [21] K. A. Mkhoyan, A. W. Contryman, J. Silcox, D. A. Stewart, G. Eda, C. Mattevi, S. Miller, M. Chhowalla, Nano Lett 2009;9(3):1058–63.
- [22]W. S. Hummers and R. E. Offeman, J. Am. Chem. Soc., 1958, 80, 1339.
- [23] D. Li, M. B. Muller, S. Gilje, R. B. Kaner and G. G. Wallace, Nat. Nanotechnol., 2008, 3, 101-105.